Advanced Structural Mechanics 1 (2023) 115-121

Advanced Structural Mechanics

Journal homepage: http://asm.sku.ac.ir

Arrhenius type constitutive equation for extruded plate of AlMg6 alloy using plane strain compression test

Javad Rasti[a,*] , Masoud Abolghasemi[b]

[a]*Assistant professor, Department of Mechanical Engineering, Qom University of Technology (QUT), Qom, P.O. Box: 37195-1519, Iran.*
[b]*MSc Student, Department of Mechanical Engineering, Qom University of Technology (QUT), Qom, P.O. Box: 37195-1519, Iran.*

Article received: 2023/ 01/ 16, Article revised: 2023/ 02/ 18, Article accepted: 2023/ 02/ 20

ABSTRACT

The traditional and most common aluminum magnesium (Al-Mg) alloys are series 5000 and 6000 which have up to a maximum value of 4.5% Mg. The presence of magnesium elements in these alloys increases the strength and hardness, but, on the other hand, intensifies the intergranular corrosion. Recently, high-strength Al-Mg alloys have been developed with the addition of > 6% Mg, resulting in higher strength and softness. The weakness of these alloys due to higher sensitivity to intergranular corrosion can be decreased by thermomechanical treatment or hot forming. The present research aims to investigate the behavior of AlMg6 alloy and provide a constitutive model based on the plane strain compression test. For this purpose, a special fixture is designed and built with proper dimensional and geometrical tolerance. The experiments are carried out at temperatures of 30-140°C and strain rates of 0.002-0.006 s^{-1}. From the obtained flow curves, the maximum stresses are determined and used in Arrhenius expression to extract the constants of the constitutive equation. The results of this model are in good agreement with the experimental ones and therefore it can be used in the modeling and simulation of deformation processes that require the constitutive equation of this alloy.

Keywords: Al-Mg alloy; Constitutive equation; Flow curve; Plane strain compression test.

1. Introduction

Nowadays, the thermomechanical process is used as an effective technology to control the microstructure and mechanical properties in various alloys. This process refers to various metal forming processes that involve careful control of thermal and deformation conditions (by means of temperature, strain rate, and strain) to achieve products with required shape specifications and good properties. Constitutive equations can give us information about the

* Corresponding author at: Department of Mechanical Engineering, Qom University of Technology (QUT), Qom, Iran.
E-mail address: rasti@qut.ac.ir
DOI: 10.22034/asm.2023.14224.1012: https://asm.sku.ac.ir/article_11391.html

behavior of material during deformation processes. In these equations, the relationship between measurable parameters such as stress, strain, temperature and strain rate are expressed in the framework of mathematical functions [1, 2].

Aluminum magnesium alloys of 5000 and 6000 series are known as common Al-Mg alloys. The presence of magnesium increases the strength, but on the other hand, aggravates the intergranular corrosion [3]. In these alloys, due to the strong reaction of magnesium with atmosphere and oxidation, the addition of >4.5% magnesium has been very difficult, however, recently Choi et al. [4] have developed a Mg+Al_2Ca master alloy by making a stable CaO/MgO mixed layer on which no significant oxidation occurred, and therefore, they could cast alloys with magnesium up to 9%. These newly developed Al-Mg alloys with enhanced strength and ductility would be promised alloys, especially for aerospace industry.

Different constitutive equations have been proposed so far by various researchers. Some of them can be seen in Table 1. Since these equations correlate the flow stress with temperature, strain, and strain rate, finding the proper equation and then related parameters is tedious, difficult and time-consuming.

Among these equations, the sine hyperbolic Arrhenius type equation was used extensively for the modeling of the characteristic stresses as a function of the Zener–Hollomon parameter (Z) [9-12, 17, 18].

$$Z = \dot{\varepsilon}\exp(Q_{\text{def}}/RT) = A\left(\sinh(\alpha\sigma)\right)^n \text{ or} \qquad (1)$$
$$\dot{\varepsilon} = A\left(\sinh(\alpha\sigma)\right)^n \exp(-Q_{\text{def}}/RT)$$

Where $\dot{\varepsilon}$ is the strain rate (s^{-1}), A, α and n are constants independent of temperature, σ is the characteristic stress (MPa), Q_{def} is the hot deformation activation energy (J mol^{-1}), R is the gas constant and T is the absolute temperature (K) of deformation. By mathematical manipulation, the flow stress may be rewritten as a function of Z as follows:

Table 1. Different constitutive equations for the modelling of flow curves.

Field Backofen (FB) [1]	$\sigma = K\varepsilon^n\dot{\varepsilon}^m \qquad K = f(T,\dot{\varepsilon}), n = g(T,\dot{\varepsilon}), m = h(T)$
Modified FB [2,5]	$\sigma = K\varepsilon^n\dot{\varepsilon}^m \exp(\mathrm{b}T + \mathrm{s}\varepsilon) \qquad n = f(T,\dot{\varepsilon}), m = g(T), K, b, s = \text{const.}$
Johnson Cook (JC) [6]	$\sigma = (A + B\varepsilon^n)\left[1 + C\ln\left(\frac{\dot{\varepsilon}}{\dot{\varepsilon}_0}\right)\right]\left[1 - \left(\frac{T-T_r}{T_m-T_r}\right)^m\right],\ A, B, n, C, \dot{\varepsilon}_0, T_r, T_m$=const.
Modified JC [7]	$\sigma = (A_0 + A_1\varepsilon + A_2\varepsilon^2)\left(1 + D_1\left(\frac{\dot{\varepsilon}}{\dot{\varepsilon}_0}\right)\right)\exp\left[\left(\lambda_1 + \lambda_2\ln\left(\frac{\dot{\varepsilon}}{\dot{\varepsilon}_0}\right)\right)(T - T_r)\right]$ $A_0, A_1, A_2, D_1, \dot{\varepsilon}_0, \lambda_1, \lambda_2, T_r = \text{const.}$
JC with grain size effect [8]	$\sigma = (A + B\varepsilon^n)\left[1 + \lambda\left(\frac{d}{d_0}\right)\right]\left[1 + C_1\ln\left(\frac{\dot{\varepsilon}}{\dot{\varepsilon}_0}\right)\right]\exp\left[\left(f\left(\frac{d}{d_0}\right) + C_1\ln\left(\frac{\dot{\varepsilon}}{\dot{\varepsilon}_0}\right)\right)(T - T_r)\right]$
Arrhenius (Arr) [9-12]	$Z = \dot{\varepsilon}\exp(Q_{\text{def}}/RT) = \begin{cases} B\,{\sigma_{\mathrm{P}}}^{n'} \\ A'\exp(\beta\sigma_{\mathrm{P}}) \\ A\left(\sinh(\alpha\sigma_{\mathrm{P}})\right)^n \end{cases} Q_{\text{def}}, B, n', A', \beta, A, \alpha, n = \text{const. or } f(\varepsilon), R = \text{gas const.}$
Zerilli Armstrong (ZA) [13]	$\sigma = c_0 + B_0\varepsilon^n\exp(-\beta_0 T + \beta_1 \mathrm{T}\ln\dot{\varepsilon}),$ n=0.5 in original work
Modified ZA [14]	$\sigma = (A_0 + A_1\varepsilon + A_2\varepsilon^2 + A_3\varepsilon^3)\times$ $\exp\left[-(B_0 + B_1\varepsilon + B_2\varepsilon^2 + B_3\varepsilon^3)(T - T_r)\right.$ $\left. + (C_0 + C_1(T - T_r) + C_2(T - T_r)^2 + C_3(T - T_r)^3)\ln\left(\frac{\dot{\varepsilon}}{\dot{\varepsilon}_0}\right)\right]$
Hansel Spittle (HS) [15]	$\sigma = A\exp(m_1 T)\varepsilon^{m_2}\dot{\varepsilon}^{m_3}\exp(m_4/\varepsilon)(1+\varepsilon)^{m_5 T}\exp(m_6\varepsilon)\dot{\varepsilon}^{m_7 T}T^{m_8}$
Voyiadjis Abed (VA) [16]	$\sigma = (c_1 + c_2\varepsilon^{c_3}) + c_4\left[1 - \left[-c_5 T\ln\left(\frac{\dot{\varepsilon}}{\dot{\varepsilon}_0}\right)\right]^{1/q_1}\right]^{1/q_2} + c_6\varepsilon^{c_7}\left[1 - \left[-c_5 T\ln\left(\frac{\dot{\varepsilon}}{\dot{\varepsilon}_0}\right)\right]^{1/q_1}\right]^{1/q_2}$

$$\sigma = \frac{1}{\alpha}\ln\left\{\left(\frac{Z}{A}\right)^{1/n} + \left[\left(\frac{Z}{A}\right)^{2/n} + 1\right]^{1/2}\right\} \quad (2)$$

Various tests are used in the evaluation of material constitutive behavior: uniaxial and biaxial tensile tests, blow forming tests, torsion tests and compression tests (ring compression, plane strain compression). The type of a test should generally correspond to the stress strain mode realized in the simulated forming process. The plane strain compression test (PSCT) is generally adopted for studies of a material flow behavior during flat rolling due to the fact that the stress-strain mode corresponding to flat rolling is very similar to the ideal plane strain compression [19, 20].

2. Materials and Method

In order to determine the constitutive equation of Al-Mg6 alloy with the plane strain compression test, an apparatus is made by the configuration shown in Fig. 1, and set between the anvils of the 25-ton uniaxial tensile test (model of STM250 belongs to Santam Company).

The following inequalities must be satisfied for the PSCT.

$$2 \le \frac{b}{t} \le 4 \quad , \quad 5 \le \frac{w}{b} \le 12 \quad (3)$$

Chemical composition of the alloy AlMg6 used in this study is as follows:

Samples with the length and width of 20 and 40 mm were cut from the rolled sheet of AlMg6 alloy with the thickness of 2 mm. All samples were annealed before test at temperature of 400°C for 30 minutes. During the test, the thickness of the material reduced up to 1 mm, which is equal to strain of about 0.69. Tests were performed at temperatures of 30, 70, and 140°C and strain rates of 0.002, 0.004, and 0.006 s^{-1}. The method subscribed in Ref. [21] was used for extracting the equivalent stress–equivalent strain curve ($\bar{\sigma}\ vs.\ \bar{\varepsilon}$) from load-displacement curve. The width of the planes is 6 mm. The Arrhenius constitutive equation of Eqs. (1) and (2) are then used for the modeling of experimental flow stresses.

Table 2. Chemical composition of AlMg6 alloy used in this research.

Alloying element		Si	Fe	Cu	Mn	Mg	Cr	Zn	Ti
AlMg6	Nominal value	<0.4	<0.4	<0.1	0.15-0.2	5.8-6.2	0.05-0.08	<0.25	0.02-0.05
	Real value	0.055	0.12	0.001	0.17	5.87	0.06	0.001	0.04

Fig. 1. An apparatus made for plane strain compression test.

Although the tensile test apparatus is equipped with the electrical furnace, a new heating tool must be applied to heat the samples due to the large dimension of the fixture. Therefore, two ideas are examined; the first is the use of industrial drier and the second is the surveying of combustion gasses from oxyacetylene flame (Fig. 2). In this study, the second idea is employed.

3. Results and Discussion

The flow curves obtained from experimental load-displacement diagrams based on the method of Ref. [21] at different conditions are shown in Fig. 3.

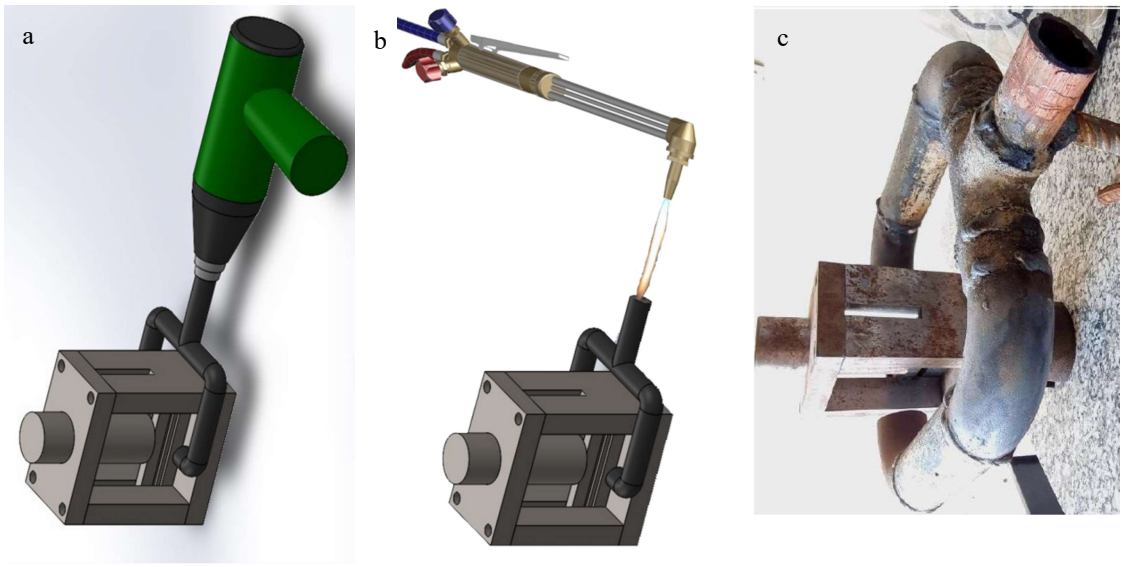

Fig. 2. Two conceptual design for heating of samples (a) heating by industrial drier; (b) heating by Oxy-acetylene torch; (c) Welded pipes for transferring hot combustion gases to the sample.

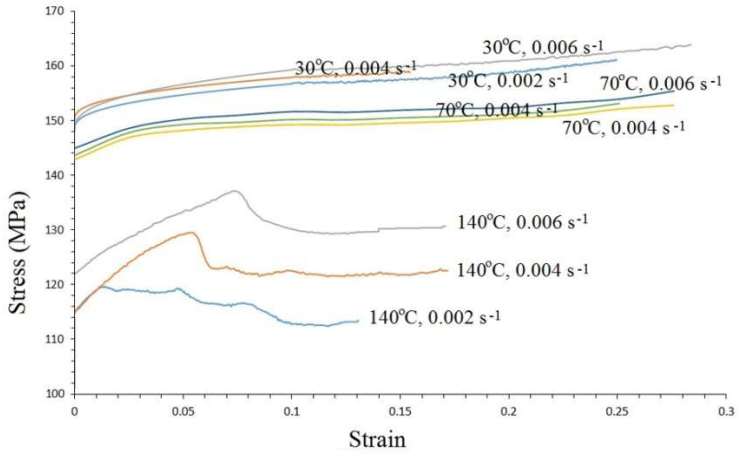

Fig. 3. Flow stress of Al-Mg6 by the plane strain compression test at different conditions.

As can be seen in Fig. 1, the flow curves at 140 undergo DRX, i.e., they reach the peak stress after an initial work hardening and then rapid work softening has occurred. Deformation at lower temperatures could result in no evidence of DRX. Thus, a high strain hardening effect was observed.

To model the stress strain curves, peak stresses were selected. Therefore, 9 stress values were obtained at different temperatures and strain rates (Table 3).

The sine hyperbolic Arrhenius type Eq. (1) was used for modeling of these stresses, on the other word, the parameters A, n, α, and Q_{def} must be determined.

The sine hyperbolic Eq. (1) is fitted for the peak stresses as follows:

$$\ln(\dot{\varepsilon}) = \ln(A) + n.\ln[\sinh(\alpha\sigma)] - Q_{\text{def}}/RT \tag{4}$$

Supposing the $\sinh(\alpha\sigma) \cong \exp(\alpha\sigma)/2$ for $\alpha\sigma > 1.2$ gives:

$$\ln(\dot{\varepsilon}) = \ln(A') + \beta\sigma - Q_{\text{def}}/RT \ , \ \beta = n\alpha \tag{5}$$

Furthermore, by regarding the $\sinh(\alpha\sigma) \cong \alpha\sigma$ for $\alpha\sigma < 0.8$

$$\ln(\dot{\varepsilon}) = \ln(A'') + n'\ln(\sigma) - Q_{\text{def}}/RT \tag{6}$$

First, by supposing the value of $\alpha = 0.001$, we can obtain n from Eq. (4) using plot of $\ln(\dot{\varepsilon}) \ vs. \ \ln[sinh(\alpha\sigma)]$ at constant temperatures. Then, using the Eq. (5) and plotting $\ln(\dot{\varepsilon}) \ vs. \ \sigma$, we can obtain $\beta = n\alpha$, which may be used to recalculate α for substitution in Eq. (4) to obtain again n, and continue this cycle to acquire correct n and α.

To identify the activation energy of deformation Q_{def}, we can use the following relation:

$$\ln[\sinh(\alpha\sigma)] = -\ln(A''') + \ln(\dot{\varepsilon})/n + Q_{\text{def}}/nRT \tag{7}$$

Now, with plotting $\ln[\sinh(\alpha\sigma)]$ vs. $1/T$, The slope of the graph is equal to Q_{def}/nR ($R = 8.314$ J/mol). Finally, the Eq. (1) can be rewritten as follows:

$$\ln(Z) = \ln(A) + n \ \ln[\sinh(\alpha\sigma)] \tag{8}$$

The value of $\ln(A)$ would be y-intercept of $\ln(Z)$ vs. $\ln[\sinh(\alpha\sigma)]$. This trend can be seen in Fig. 4. Regarding the plots of Fig. 4, the values of n, α, Q and A are obtained respectively as n=3.5, α=0.0075, Q=84300 J/mol, and $A=5.7\times10^{14}$.

The comparison of the experimental stresses with the stresses obtained from the Arrhenius relationship is shown in Fig. 5. As can be seen the Arrhenius equation agrees well with the experimental results, and therefore it can be used to predict the peak stresses in the other temperature and strain rate conditions.

Table 3. Peak stresses at different temperatures and strain rates.

Test No.	Temperature (°C)	Strain rate (s^{-1})	Peak stress (MPa)
1	30	2×10^{-3}	161.7
2	70	2×10^{-3}	145.9
3	140	2×10^{-3}	135.3
4	30	4×10^{-3}	162.6
5	70	4×10^{-3}	146.6
6	140	4×10^{-3}	136.5
7	30	6×10^{-3}	163.8
8	70	6×10^{-3}	148.5
9	140	6×10^{-3}	137.3

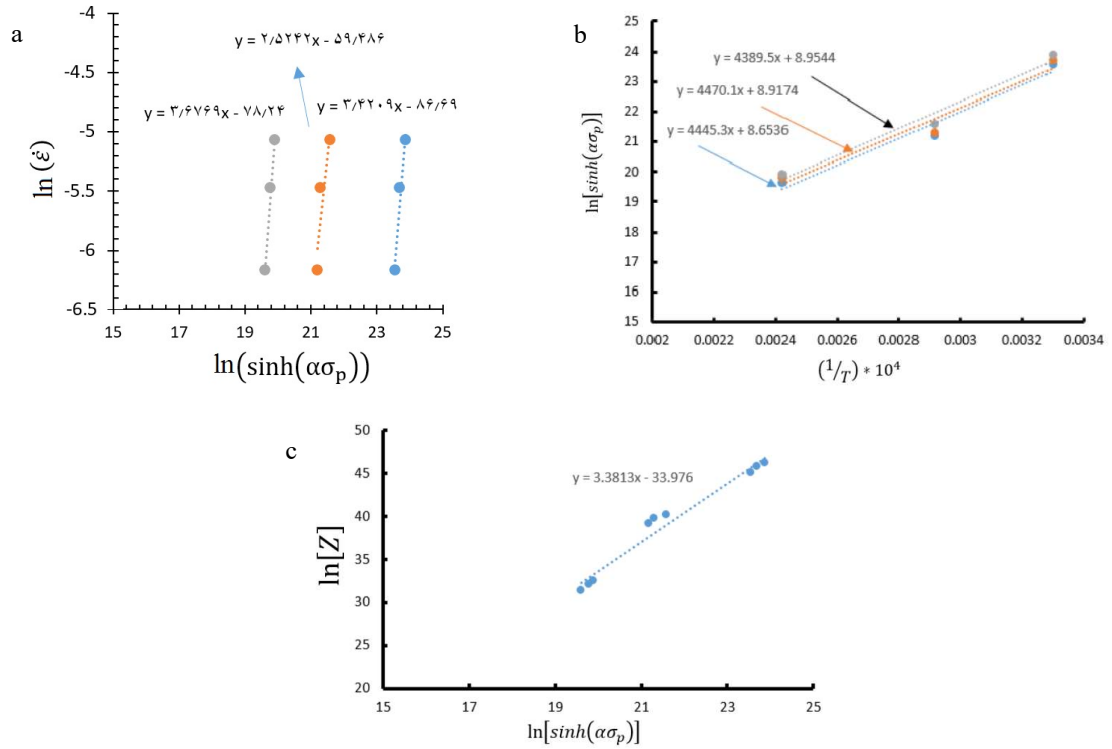

Fig. 4. Determination of Arrhenius constitutive equation parameters at peak stress (a) Determining n from the slope of the diagram according to Eq. (4) ; (b) Determining Q_{def}/nR from the slope of the diagram according to Eq. (7) ; (c) Determining $\ln(A)$ from the slope of the diagram according to Eq. (8).

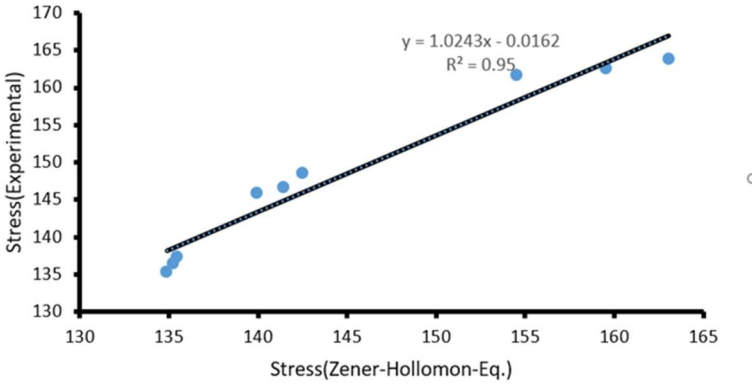

Fig. 5. Comparison between the experimental peak stresses and those obtained via Arrhenius model.

4. Conclusions

In this work, the flow behavior of new extruded aluminum magnesium alloy AlMg6 was studied at temperature ranges of 30-140 °C and strain rates of 0.002-0.006 s^{-1} and the following results were obtained:

1- To resemble the rolling situation, a plane strain compression test was carried out at different conditions.

2- A special fixture was designed and built with proper dimensional and geometrical tolerance so that the plane strain compression test can be accomplished with the universal uniaxial tension/compression test.
3- The combustion gases from oxyacetylene flame were used for heating samples.
4- The peak stresses were determined from the experimental flow curves and used into Arrhenius equation to calculate the constants of the Zener-Hollomon equation.
5- The values of n=3.5, α=0.0075, Q=84300 J/mol, and A=5.7+E14 were obtained.
6- The model could satisfactorily coincide with the experimental results and therefore can be employed for predicting flow stress of this alloy during forming processes.

Acknowledgements

Authors would like to thank the Vice President of Education and Research, Qom University of Technology (QUT) for granting this study.

References

[1] Fields, D.S., Backofen, W.A., 1957. Determination of Strain Hardening Characteristics by Torsion Testing. Proceedings-American Society of Testing Materials. 57, 1259-1272.
[2] Nitin, K., Hansoge, N.K., Amit, K.G., Swadesh, K.S., 2018. Study of Hot Deformation Behaviour Using Phenomenological Based Constitutive Model for Austenitic Stainless Steel 316. Materials Today: Proceedings 5. 4870-4877.
[3] Vargel, C., 2020. Corrosion of Aluminium. Elsevier, 2nd Ed., https://doi.org/10.1016/B978-0-08-099925-8.00033-8
[4] Choi, K.H., Kim, B.H., Lee, D.B., Yang, S.Y., Kim, N.S., Ha, S.H., Yoon, Y.O., Lim, H.-K., Kim, S.K., 2021. Effect of Combined Extrusion and Rolling Parameters on Mechanical and Corrosion Properties of New High Strength Al-Mg Alloy. Metals. 11, 445.
[5] Ji, G., Li, L., Qin, F., Zhu, L., Li, Q., 2017. Comparative study of phenomenological constitutive equations for an as-rolled M50NiL steel during hot deformation. Jounal of Alloy Compounds. 695, 2389-2399.
[6] Lin, Y.C., Chen, X., 2011. A critical review of experimental results and constitutive descriptions for metals and alloys in hot working. Materials and Design. 32, 1733-1759.
[7] Lu, W.J., Hou, L.Q., Zhang, X.Q., Xu, P.M., 2016. Thermal deformation properties and Johnson-Cook models for superaustenitic stainless steel. Journal of Plasticity Engeering. 23, 125-130.
[8] Rezaei-Ashtiani, H.R., Shayanpoor, A.A., 2021. New constitutive equation utilizing grain size for modeling of hot deformation behavior of AA1070 aluminum .Transaction of Nonferrous Metals Society of China. 31, 345−357.
[9] Ban, Y., Zhang, Y., Jia, Y., Tian, B., Volinsky, A.A., Zhang, X., Zhang, Q., Geng, Y., Liu, Y., Li, X., 2020. Effects of Cr addition on the constitutive equation and precipitated phases of copper alloy during hot deformation. Materials and Design. 191, 108613.
[10] Aliakbari-Sani, S., Ebrahimi, G.R., Vafaeenezhad, H., Kiani-Rashid, A.R., 2018. Modeling of hot deformation behavior and prediction of flow stress of a magnesium alloy using constitutive equation and artificial neural network (ANN) model. Journal of Magnesium and Alloys. 6, 134–144.
[11] Wu, H., Yang, J., Zhu, F., Wu, C., 2013. Hot compressive flow stress modeling of homogenized AZ61 Mg alloy using strain-dependent constitutive equations. Materials Science and Engineering A. 574, 17–24.
[12] Dai, Q., Deng, Y., Tang, J., Wang, Y., 2019. Deformation characteristics and strain-compensated constitutive equation for AA5083 aluminum alloy under hot compression. Transaction of Nonferrous Metals Society of China. 29, 2252−2261.
[13] Zerilli, F.J., Armstrong, R.W., 1987. Dislocation-mechanics-based constitutive relations for material dynamics calculations. Journal of Applied Physics. 61, 1816-1825.
[14] Huang, X., Wang, B., Zang, Y., Ji, H., Guan, B., Li, Y., Tang, X., 2020. Constitutive relationships of 21-4 N heat-resistant steel for the hot forging process. Journal of Materials Research and Technolonogy. 9(6), 13575–13593.
[15] Hensel, A., Spittel, T., 1978. Kraft- und Arbeitsbedarf bildsamer Formgebungsverfahren. VEB Deutscher Verlag fur Grundstoffindustrie. Leipzig. ISBN: 5991fb6601cdf532e1408fc6566c7635
[16] Tabei, A., Abed, F.H., Voyiadjis, G.Z., Garmestani, H., 2017. Constitutive Modeling of Ti-6Al-4V at a Wide Range of Temperatures and Strain Rates. European Journal of Mechanics /A Solids. 63, 128-135.
[17] Zener, C., Hollomon, H., 1969. Effect of strain-rate upon the plastic flow of steel. Journal of Applied Physics. 15, 22–27.
[18] Jonas, J.J., Sellars, C.M., Tegart, M.W.J., 1969. Strength and structure under hot working conditions. International of Metals Revision. 14, 1–24.
[19] Lenard, J.G., Karagiozis, A.N., 1989. Accuracy of high-temperature, constant rate of strain flow curves: In Factors That Affect the Precision of Mechanical Tests ASTM International. 206-216.
[20] Pietrzyk, M., Lenard, J.G., Dalton, G.M., 1993. A study of the plane strain compression test. CIRP annals. 42(1), 331-334.
[21] Loveday, M.S., Mahon, G.J., Roebuck, B., Lacey, A.J., Palmiere, E.J., Sellars, C.M., van der Winden, M.R., 2006. Measurement of flow stress in hot plane strain compression tests. Materials at High Temperatures. 23(2), 85-118